Journal of Radiation Research, Vol. 63, No. 5, 2022, pp. 741–748
https://doi.org/10.1093/jrr/rrac034
Advance Access Publication: 11 July 2022

Clinical application and accuracy assessment of imaging-based surgical navigation guided ^{125}I interstitial brachytherapy in deep head and neck regions

Guohao Zhang[1], Zhiyuan Wu[2], Wenting Yu[3], Xiaoming Lyu[1], Wenjie Wu[1], Yi Fan[4], Yong Wang[5], Lei Zheng[1], Mingwei Huang[1], Yi Zhang[1], Chuanbin Guo[1] and Jianguo Zhang[1,*]

[1]Department of Oral and Maxillofacial Surgery, Peking University School and Hospital of Stomatology & National Center of Stomatology & National Clinical Research Center for Oral Diseases & National Engineering Research Center of Oral Biomaterials and Digital Medical Devices, Beijing 100081, PR China
[2]Department of Oral and Maxillofacial Surgery, Fujian Provincial Hospital, Fuzhou 350001, PR China
[3]Department of Orthodontics, Beijing Stomatological Hospital, School of Stomatology, Capital Medical University, Beijing 100050, PR China
[4]Department of Orthodontics, Peking University School and Hospital of Stomatology & National Center of Stomatology & National Clinical Research Center for Oral Diseases & National Engineering Research Center of Oral Biomaterials and Digital Medical Devices & Beijing Key Laboratory of Digital Stomatology, Beijing 100081, PR China
[5]Center of Digital Dentistry, Peking University School and Hospital of Stomatology & National Center of Stomatology & National Clinical Research Center for Oral Diseases & National Engineering Research Center of Oral Biomaterials and Digital Medical Devices & Beijing Key Laboratory of Digital Stomatology & Research Center of Engineering and Technology for Computerized Dentistry Ministry of Health, Beijing 100081, PR China
*Corresponding author. Department of Oral and Maxillofacial Surgery, Peking University School and Hospital of Stomatology & National Center of Stomatology & National Clinical Research Center for Oral Diseases & National Engineering Research Center of Oral Biomaterials and Digital Medical Devices, No. 22 Zhongguancun South Avenue, Haidian District, Beijing 100081, PR China. Email: rszhang@126.com, Fax Number: 86-10-82195701
(Received 18 February 2022; revised 26 April 2022; editorial decision 18 May 2022)

ABSTRACT

Brachytherapy has the advantages of being minimally invasive and highly conformal, and it achieves good results in head and neck tumors. To precisely implant the radioactive seeds according to the preplan in deep head and neck regions, the surgical navigation is applied. This study aims to explore the clinical application and accuracy of imaging-based surgical navigation-guided ^{125}I interstitial brachytherapy in terms of seed position. We included 41 patients with tumors in deep head and neck regions. The brachytherapy treatment plan was designed, and the preplanned data were transferred to the navigation system. Needle implantation and seed delivery were performed under surgical navigation system guidance with or without the combination of individual template. The treatment accuracy was evaluated by comparing seed cluster locations between the preoperative treatment plan and the postoperative treatment outcome. A total of 2879 seeds were delivered. The range, mean and median distances between the geometric centers of the preoperative seed point clusters and the postoperative seed point clusters were 0.8–10.5 mm, 4.5 ± 2.3 mm and 4.1 mm, respectively. The differences between preoperative and postoperative volumes of the minimum bounding box of seed point clusters were nonsignificant. In conclusion, the imaging-based surgical navigation system is a promising clinical tool to provide the preplanned data for interstitial brachytherapy intraoperatively, and it is feasible and accurate for the real-time guidance of needle implantation and seed delivery in deep head and neck regions.

Keywords: accuracy; navigation; brachytherapy; head and neck

INTRODUCTION

^{125}I interstitial brachytherapy is an effective and widely accepted method for treating tumors [1–5]. One of the advantages of interstitial brachytherapy is that it allows the delivery of high radiation doses to the tumors while reducing the radiation dose to normal adjacent structures [6]. The precise delivery of radioactive seeds according to the treatment plan is critical to the success of brachytherapy.

Tumors that involve deep head and neck regions are quite challenging to manage, as injuries to the organs at risk (e.g. brain tissue, eyeballs, carotid artery, jugular vein) may cause serious complications [7]. As an effective alternative treatment, ^{125}I interstitial brachytherapy, with the advantages of being minimally invasive and highly conformal, achieves good results in deep head and neck tumors [8, 9]. However, as the anatomical structures of the head and neck are complex, performing brachytherapy in these regions is difficult. To ensure appropriate dose distribution and seed stability, and avoid puncture injuries and radiation damage to neighboring critical tissues, the treatment plan must be optimally made and transferred to the implantation procedure to guide needle insertion and seed delivery.

The 3D-printed individual template, which can transfer the preplanned data to the operation procedure, has been designed and applied for guiding head and neck brachytherapy [10]. And the accuracy result of the individual template guidance in terms of the mean entrance point distance deviation was 1.2 mm [11]. With the development of computer-assisted techniques, surgical navigation is being widely applied and has improved the accuracy and outcomes of surgery in the head and neck regions [12–15]. The principle of surgical navigation systems in medicine is to guide the accurate placement of surgical instruments and monitor their trajectories in the patient's body by processing and displaying appropriate information available in pre- or intraoperative images [16]. To precisely implant the radioactive seeds according to the preplan, surgical navigation is applied in brachytherapy. However, the deformation of soft tissues during implantation may impact the accuracy of navigation guidance [17]. The craniofacial bones in head and neck regions remain in a relatively stable position, which may be beneficial for the navigation system to precisely locate the target area and guide interstitial brachytherapy. A previous pilot study demonstrated that the navigation system with the combination of the individual template guidance is safe and feasible in head and neck brachytherapy. And the mean target point deviation was 5.2 mm, which represented the accuracy result of the needle tip position under guidance [18]. However, the position of the seeds, which are delivered under guidance via the needles, has not been well studied.

This study aims to explore the clinical application and accuracy of imaging-based surgical navigation-guided ^{125}I interstitial brachytherapy in deep head and neck regions in terms of seed position.

MATERIALS AND METHODS

Patients

From January 2011 to October 2021, we included 41 patients who received imaging-based surgical navigation-guided ^{125}I interstitial brachytherapy in this study. Locally advanced tumors in head and neck regions were pathologically diagnosed in all patients prior to brachytherapy, and the patients had never received radioactive seed implantation before. The baseline information of the patients and treatments are shown in Table 1. All the tumors involved the skull base, and they also involved the infratemporal fossa, orbital floor, maxilla, mandible, deep lobe of parotid gland, or parapharyngeal region. All patients signed informed consent forms before treatment. The study was approved by the Ethical Committee of Peking University School and Hospital of Stomatology (No. PKUSSIRB-202171213).

Table 1. Information of the patients

Characteristic	Number
Gender	
Male	21
Female	20
Age, mean (years)	
2–18	15
18–80	26
Pathological diagnosis	
Adenoid cystic carcinoma	11
Rhabdomyosarcoma	7
Myoepithelial carcinoma	3
Myofibroma	3
Ewing sarcoma	2
Mucoepidermoid carcinoma	2
Synovial sarcoma	2
Desmoid-type fibromatosis	1
Acinic cell carcinoma	1
Epithelial-myoepithelial carcinoma	1
Leiomyosarcoma	1
Malignant pleomorphic adenoma	1
Malignant rhabdoid tumor	1
Meningioma	1
Osteosarcoma	1
Polymorphous low-grade adenocarcinoma	1
Squamous cell carcinoma	1
Synovial chondrosarcoma	1
Greatest dimension of tumor (cm)	
0–4	4
4–8	29
8–12	8
Guidance type	
Navigation	6
Navigation and individual template	35

Brachytherapy preplanning

A preoperative spiral computed tomography (CT) scan with a slice thickness of 0.75 mm was obtained for all patients. The treatment plan of brachytherapy was made by a brachytherapy treatment planning system (BTPS; Beijing Astro Technology Ltd Co., Beijing, China) based on CT images. The planning target volume (PTV) was delineated. Radioactivity of the ^{125}I seed (model 6711, China Institute of Atomic Energy, Beijing, China) was 0.5–0.7 mCi. The seed was 4.5 mm in

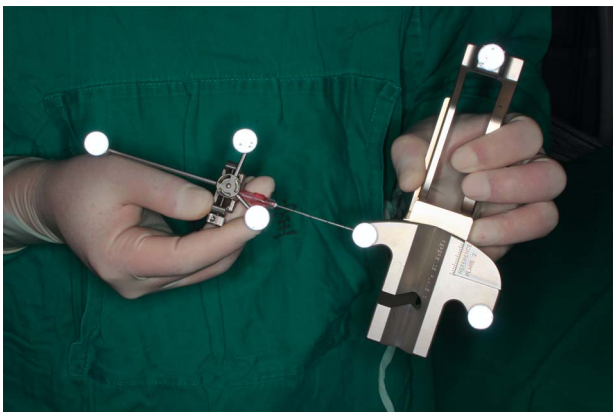

Fig. 1. The needle with three reflective marker spheres at the needle end was registered to the surgical navigation system.

length and 0.8 mm in diameter. The matched peripheral dose (MPD) was 80–120 Gy, which was determined according to the treatment strategy of the patient (brachytherapy alone, surgery combined with brachytherapy, brachytherapy for patients with prior radiotherapy), histological type and stage of the tumor, and the adjacent structures of the target area. The prescribed dose was set as the MPD encompassing the PTV. The preplanned data, including the coordinates of implant needles and seeds, were saved and exported.

The digital preparation and guidance

According to the type of guidance, the patients were divided into two groups: the surgical navigation system guidance group and the navigation system combined with individual template guidance group.

In the group of surgical navigation system guidance, we imported the CT images of the patient in DICOM format into iPlan CMF software (BrainLAB, Feldkirchen, Germany) to make the navigation plan. The needle trajectory was designed by the operators based on the location of the needles in BTPS. The position of the preplanned deepest seed in one trajectory was set as the target point, and the intersection of the preplanned trajectory and skin was set as the entrance point. To make the organs at risk (e.g. carotid artery, jugular vein) visible during implantation, they were marked with different colors according to the CT data. Then the navigation plan was transferred to the surgical navigation system, which consists of the localization system and the computer platform. The two infrared cameras on the localizer can detect the spatial locations of the reflective marker spheres, which are fixed to the surgical instruments and the reference frame. The computer monitor is used for real-time visualization of the relative spatial locations of the surgical instruments and the patient anatomy. Under general anesthesia, the reference frame with three reflective marker spheres was fixed to the patient's head. Afterward, the operator used the Z-touch wireless laser pointer to perform navigation system registration through facial surface scanning. And then the needle with reflective marker spheres was registered to the surgical navigation system (Fig. 1). The operator inserted the needles with the guidance of the images on the computer monitor. The orientation and depth of the needles were adjusted according to the relative spatial location of the needles and trajectories on the navigation screen (Fig. 2). After the needle reaching the target point in one trajectory, the deepest seed was delivered. Then we pulled out the needle at the preplanned insertion depth and delivered the other seeds in this trajectory.

The surgical navigation system and the individual template were combined for brachytherapy guidance in the other group. The individual template was designed and fabricated based on CT and preplanned needle data [10, 11]. Applying Mimics software (Materialise, Leuven, Belgium), we reconstructed the appearance of the head and neck region and the needle trajectories using the preoperative CT images and the coordinates of preplanned needles. The appearance of the individual template was designed according to the 3D data of the head and neck using Geomagic Studio (3D Systems, Morrisville, NC, USA), ideally covering landmarks such as the ear, the nose or the zygoma to facilitate the correct placement of the template. The cylinder with an inner hole was designed according to the preplanned needle data to constrain the entrance point and direction of the needle. On the basis of the design, the individual template was constructed from medial light-cured resin. In order to make the preplanned needle trajectories visible during operation, we applied the coordinates of the preplanned needles in BTPS to make digital trajectory model using Geomagic Studio. The tip of the trajectory model, which represented the position of the deepest seed in a trajectory, was set as the target point. The digital model of the individual template and the digital trajectory models were merged (Fig. 3) and imported into the iPlan CMF software [18]. During operation, the individual template was placed in the planned position under the guidance of surgical navigation, and the navigation probe was used to check the position of the cylinder before needle puncture (Fig. 4). Then the needles were inserted via cylinders on the template (Fig. 5), and the navigation system was used for real time monitoring the needles' position (Fig. 6). After all the needles were inserted, the seeds were delivered according to the plan.

We collected the data of treatment time of the patients. The average time for delivering a seed was computed as the value of treatment time divided by the number of implanted seeds. To verify the treatment outcome, CT examination with 0.75 mm slice thickness was performed within 48 hours after seeds implantation.

Verification of the treatment

The postoperative CT data were imported into the BTPS, and the quality of the treatment was verified. The postoperative dosimetric parameters were D_{90} (the dose received by 90% of the PTV), V_{100} (the volume percentage of the PTV that received 100% of the prescribed dose) and V_{150} (the volume percentage of the PTV that received 150% of the prescribed dose).

Accuracy assessment

The treatment accuracy was evaluated by comparing seed cluster locations between the preoperative treatment plan and the postoperative treatment outcome. Using Mimics software and Geomagic Studio, the preplanned seed points were merged with the digital bone model, which was reconstructed from the preoperative CT scan. Postoperative CT was used to reconstruct the seeds and bone. Afterward, the preceding preoperative and postoperative models were imported in the same coordinate system. The positions of the two models were

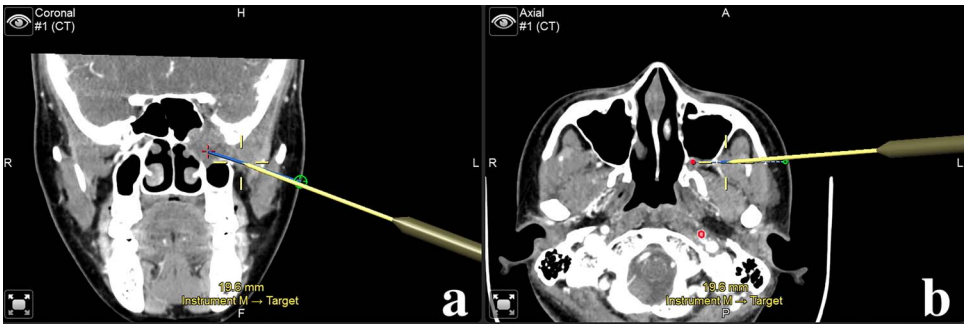

Fig. 2. The navigation monitor showed the real-time position of the preplanned entrance point (small green circle), target point (red dot), needle trajectory (blue line) and the needle that was being inserted into the skull base (yellow needle) in coronal image (a) and axial image (b) during the operation.

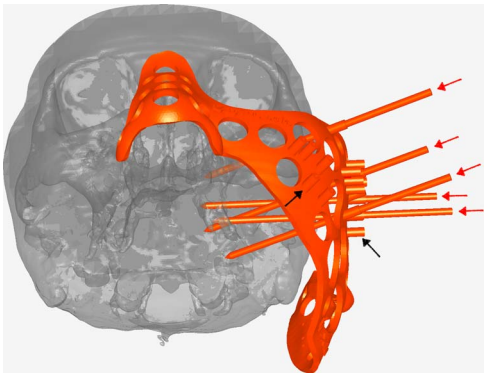

Fig. 3. The digital model of the individual template and the digital trajectory models (red arrows) were merged. The cylinders (black arrows) were designed according to the preplanned needle data to constrain the entrance point and direction of the needles.

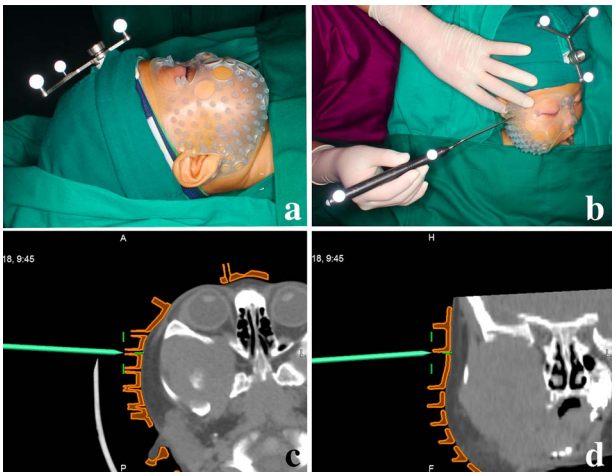

Fig. 4. The surgical navigation system and individual template were combined to guide needle implantation (a). The navigation probe was used to check the position of the cylinder on individual template (b). The navigation monitor showed the real-time position of the probe (green needle), and the digital model of individual template (orange object) in axial image (c) and coronal image (d).

matched according to the bony structures using the 'best-fit registration function' in Geomagic Studio software.

The centroid of each seed model was extracted in postoperative models. We applied the geometric center and minimum bounding box to evaluate the location of a seed point cluster (Fig. 7). The coordinate of the geometric center was determined as the average value of coordinates of each axis in a seed point cluster. The distances between the preoperative and postoperative geometric centers were calculated, representing the global deviation of the seed point clusters. The volume of the minimum bounding box, defined as the smallest-volume box including all of the points in a point cluster, was used for quantitative evaluation of the coverage of a seed point cluster. The volume was automatically calculated by the algorithm in Geomagic software for comparison [19].

Statistical analysis

SPSS (version 13.0; SPSS Inc., Chicago, USA) was used to carry out statistical analysis. The volumes of the minimum bounding box were compared between the preoperative and postoperative groups. We first used the Shapiro–Wilk test to verify whether the data were normally distributed, and $P > 0.05$ indicated that the data obeyed a normal distribution. A paired t test was applied for the comparison of normally distributed data. A nonparametric test was used for the comparison of nonnormally distributed data. The deviations of the preoperative and postoperative geometric center and volume of the minimum bounding box were compared in different groups of guidance type using the independent-samples t test. $P \leq 0.05$ was considered as statistically significant.

RESULTS

The implantations of all 41 patients were performed successfully under guidance. All the needles were implanted at the designed position, the seeds were delivered according to the plan, and no puncture-related complications occurred intraoperatively or within two weeks.

Table 2. Treatment information

Group	Greatest tumor dimension (cm)		Number of seeds per patient		Postoperative dosimetric parameters						T1 (min)	T2 (min)
					D_{90} (Gy)		V_{100} (%)		V_{150} (%)			
	Mean	Range	Mean	Range	Mean	Range	Mean	Range	Mean	Range		
A	5.4	2.9–8.7	39.7	14–82	112.0	84.3–128.4	93.2	91.1–94.6	54.7	39.8–67.1	56.5	1.4
B	6.4	3.1–10.7	75.5	19–126	117.9	90.1–131.6	92.5	90.1–95.9	55.8	40.4–68.2	84.2	1.1

A = surgical navigation system guidance group; B = surgical navigation system combined with individual template guidance group; T1 = the average treatment time of a patient; T2 = the average time for delivering a seed.

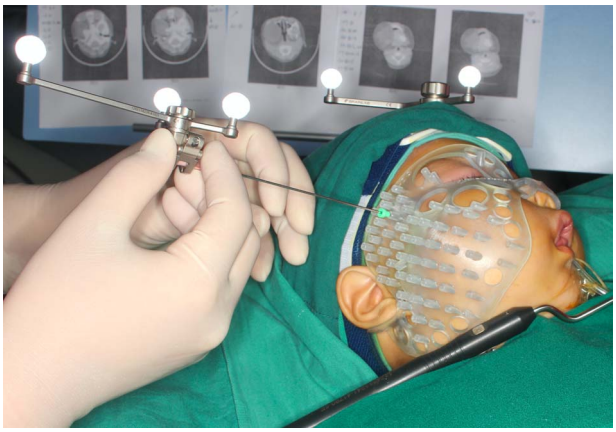

Fig. 5. The needles were inserted via cylinders on the template, and the navigation system was used for real time monitoring the needles' positions.

A total of 2879 seeds were delivered. For the postoperative evaluation of the dose distribution, the mean D_{90} were 117.0 ± 12.8 Gy (range from 84.3 Gy to 131.6 Gy), which was larger than the prescription dose for every patient. The mean V_{100} was $92.6\% \pm 1.7\%$ (range from 90.1% to 95.9%), and the mean V_{150} was $55.6\% \pm 8.9\%$ (range from 39.8% to 68.2%). The postoperative dose distributions met the treatment demands for every patient. The detailed treatment information is shown in Table 2. The average time for delivering a seed in the navigation guidance group and in the navigation combined with the individual template guidance group was 1.4 min and 1.1 min, respectively.

The accuracy assessment results showed that the range, mean and median distances between the geometric centers of the preoperative seed point clusters and the postoperative seed point clusters were 0.8–10.5 mm, 4.5 ± 2.3 mm and 4.1 mm, respectively. There was no statistically significant difference for the geometric centers' deviation between the two groups (Table 3).

The volumes of the preoperative and postoperative minimum bounding box were showed in Table 4. Using the Shapiro–Wilk test, the data of preoperative and postoperative volumes of the minimum bounding box was not normally distributed ($P < 0.05$). With the adoption of the nonparametric test (Wilcoxon test), the differences between preoperative and postoperative volumes of the minimum bounding box were nonsignificant ($P > 0.05$). And there was no statistically significant difference for the volumes' deviation of the preoperative and postoperative minimum bounding box between the two groups.

DISCUSSION

The anatomy of the head and neck is complicated and includes critical structures such as the internal jugular vein, carotid artery, brain tissues, cranial nerves and eyeballs. Head and neck tumors, especially those located in deep regions, are extremely difficult to treat by radical resection or radiotherapy, which may cause functional and esthetic damage [7]. Therefore, precision therapy with minimal invasion is required. ^{125}I interstitial brachytherapy has proven to be an effective treatment option for locally advanced head and neck tumors [4, 9]. The quality of brachytherapy depends on the coverage of the PTV and the dose distribution, which are associated with the implant geometry. The radioactive sources are implanted through percutaneous needles. Even experienced operators can hardly ensure precise seed implantation without any guidance in these high-risk regions, while avoiding bones, sinus cavities, vessels and critical structures. To guarantee therapeutic efficacy and reduce complications, real-time imaging guidance for assisting needle puncture and seed delivery is crucial. Thus, we adopted the navigation system to show the spatial position of the needles to the operator, who can then adjust the orientation and depth of needle insertion. All the preplanned needle trajectories were accomplished successfully and safely.

During brachytherapy operation procedures, image guidance can provide three-dimensional visualization of the target area as well as the implantation of the needles within the target area. The transrectal ultrasound (TRUS)-guided prostate brachytherapy has become the standard treatment [20]. CT or magnetic resonance imaging (MRI), which can enhance 3D visibility during treatment, has also been applied to guide needle insertion and radioactive seed implantation [21–23]. The navigation system is based on the synchronization of the intraoperative location of the surgical instruments with the imaging of the patient anatomy obtained previously by CT scan or MRI. Even though there are few dedicated navigation systems for brachytherapy being applied to clinical practice, some researchers have used surgical navigation systems to guide needle insertion during brachytherapy procedures [24, 25]. Ren *et al.* reported the implantation of radioactive seeds into

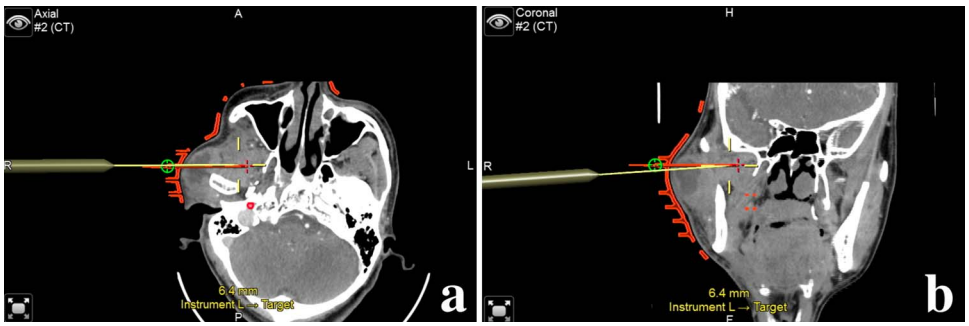

Fig. 6. On the navigation monitor, the entrance point (small green circle) represented the cylinder on the individual template (orange object) in axial image (a) and coronal image (b). The operator implanted the needle (yellow needle) through the cylinder on individual template, and finely adjusted the direction and depth of insertion along the digital trajectory model (orange line) to the target point (red dot).

Table 3. Geometric centers deviation

Group	Number of patients	Number of seeds	Deviation (mm)			
			Mean	Median	Range	SD
A	6	238	5.6	4.9	3.1–8.7	1.9
B	35	2641	4.4	3.9	0.8–10.5	2.3
Total	41	2879	4.5	4.1	0.8–10.5	2.3

A = surgical navigation system guidance group; B = surgical navigation system combined with individual template guidance group.

Table 4. Volume of the minimum bounding box of seed point cluster

Group	Preoperative (cm^3)		Postoperative (cm^3)	
	Mean	Median	Mean	Median
A	77.3	52.3	77.3	58.2
B	182.8	160.0	187.1	175.2
Total	167.3	150.9	171.0	146.8

A = surgical navigation system guidance group; B = surgical navigation system combined with individual template guidance group.

the cranial base and orbital apex with the assistance of a commercial surgical navigation system, and the navigator provided effective guidance for high-risk procedures, preventing damage to neural tissues [26]. Furthermore, researchers evaluated the accuracy of navigation system guidance by comparing the position of the preplanned needle and the actual needle. Ji *et al.* included 14 cases with tumors in the head and neck or chest. The results showed that the mean insertion point error was 1.2 mm, and the mean needle tip error was 2.7 mm [17]. Zhang *et al.* analyzed 58 needles implanted with navigation assistance in deep head and neck regions. The mean deviation of the needle tip was 5.2 mm, and postoperative dose distributions were excellent [18].

In our study, we provide a method for imaging-based surgical navigated ^{125}I interstitial brachytherapy using a commercial surgical navigation system. To transfer the radiation treatment plan to the surgical navigation system, we used commercial software such as Mimics and Geomagic to address the compatibility issues. The digital trajectory model is built and acts as a bridge between the navigation system and BTPS. Moreover, the needle is registered to the surgical system by attaching a specialized device to the end of the needle, and then it is tracked and displayed on the navigation screen. Therefore, needle implantation can be traced and corrected with the guidance of the navigation system by showing its real-time relationship to the preplanned images and the treatment plan. The results of the study showed that imaging-based surgical navigation system guided brachytherapy was feasible.

The single navigation system guidance was applied to smaller tumors which located in deep regions of the head and neck, and the needle trajectories in one case were usually designed in the same direction. As for larger tumors, the target area was reached via several puncture routes, thus the navigation system combined with individual template was applied for better controlling the position and direction of the needles. Compared to single surgical navigation guidance, the combination of the navigation and the individual template makes the implantation procedure easier. During seed delivery, the cylinders on

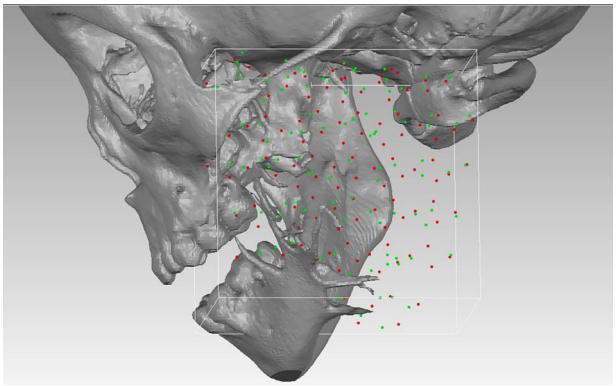

Fig. 7. The preplanned seed point cluster (red dots) and the postoperative seed point cluster (green dots) were registered in the same coordinate system for location comparison. The minimum bounding box of the seed point cluster was computed automatically and presented in Geomagic software.

the individual template can stabilize the needle orientation when the operator inserts and withdraws the needles. The results showed that the average time for delivering a seed was shorter in the navigation system combined with individual template group than in the navigation group, which may be because after the first three or four needles were placed, the individual template, which was profile matching with the craniofacial appearance of the patient, was appropriately fixed for subsequent guidance, and the operator can easily confirm other insertion points and orientations by the cylinders on the template. Furthermore, although the craniofacial bones in head and neck regions pose a barrier to needle implantation and seed delivery, the position of the bony structures and the surrounding tissues is relatively stable compared to other soft tissue areas. Since the bones can be avoided by means of computer-assisted trajectory planning, navigation combined with individual template guidance has advantages in brachytherapy of deep head and neck regions. However, for smaller tumors which means less radioactive seeds are needed to be delivered under guidance, the single navigation system guidance is more applicable for saving the procedure of preoperative preparation and intraoperative placement of the individual template. The results of postoperative dosimetric parameters showed that good postoperative dose distribution was achieved for every patient in the two groups.

To assess the accuracy of navigation system-guided brachytherapy in deep head and neck regions, we compared the overall location of preplanned seeds and postoperative seeds. The big data results showed that the mean deviation of geometric centers of the preoperative seed point clusters and the postoperative seed point clusters was 4.5 mm, and the median value was 4.1 mm. The results not only reflect the precision value of navigation-guided brachytherapy of head and neck tumors but also represent the accuracy of navigation-guided needle punctures in deep head and neck regions. Moreover, the volumes of the minimum bounding box of the preplanned and actual seed points showed no statistically significant difference, demonstrating that the treatment plans were accurately implemented under navigation guidance. There was no statistically significant difference for the geometric centers' deviation of the preoperative and postoperative seed point clusters and the volumes deviation of the preoperative and postoperative minimum bounding box between the navigation guidance group and the navigation combined with individual template guidance group.

The advantages of imaging-based surgical navigation guidance are that real-time visualization of the preplan and needle positions can be intraoperatively provided, thus the therapeutic effect and safety can be guaranteed. As a result of accurately implementing the optimized preplan, the intraoperative uncertainty is reduced. Moreover, compared with CT-guided needle placements, navigation system-guided brachytherapy is noninvasive and prevents excessive radiation exposure to the operators and patients. Some factors may influence the results of the application and accuracy evaluation of the navigation system. When puncturing the firm tissues, the deformation of the needle may cause a difference between the actual needle tip position and what the computer monitor shows. Increasing the rigidity of the needle can improve the precision of real-time navigation guidance. Furthermore, although the needle's position error is the common factor that is responsible for the loss of target area coverage in brachytherapy [27], the position of the actual seeds can also be affected by the techniques of seed implantation, the tissue swelling or shrinkage after the operation, and blood vessels in the target area which may cause seed migration [28]. In the accuracy evaluation, the implanted seeds in CT images are similar to each other in appearance. Thus, the one-to-one match and analysis between preplanned and postoperative seed points are challenging and unreliable.

In conclusion, the imaging-based surgical navigation system is a promising clinical tool to provide the preplan for interstitial brachytherapy intraoperatively, and it is feasible and accurate for the real-time guidance of needle implantation and seed delivery in deep head and neck regions.

CONFLICT OF INTEREST

The authors have no relevant conflicts of interest to disclose.

ETHICS STATEMENT

The study was approved by the Ethical Committee of Peking University School and Hospital of Stomatology (No. PKUSSIRB-202171213).

REFERENCES

1. Sylvester J, Blasko JC, Grimm P et al. Interstitial implantation techniques in prostate cancer. *J Surg Oncol* 1997;66:65–75.
2. Keller B, Sankreacha R, Rakovitch E et al. A permanent breast seed implant as partial breast radiation therapy for early-stage patients: a comparison of palladium-103 and iodine-125 isotopes based on radiation safety considerations. *Int J Radiat Oncol Biol Phys* 2005;62:358–65.
3. Jiang Y, Meng N, Wang JJ et al. CT-guided iodine-125 seed permanent implantation for recurrent head and neck cancers. *Radiat Oncol* 2010;5:68.
4. Zheng L, Zhang JG, Zhang J et al. Preliminary results of ^{125}I interstitial brachytherapy for locally recurrent parotid gland cancer in previously irradiated patients. *Head Neck* 2012;34:1445–9.

5. Glaser MG, Leslie MD, Coles I et al. Iodine seeds in the treatment of slowly proliferating tumours in the head and neck region. *Clin Oncol (R Coll Radiol)* 1995;7:106–9.
6. Langley S, Laing R. Prostate brachytherapy has come of age: a review of the technique and results. *BJU Int* 2002;89:241–9.
7. Ramakrishna R, Raza SM, Kupferman M et al. Adenoid cystic carcinoma of the skull base: results with an aggressive multidisciplinary approach. *J Neurosurg* 2015;124:115–21.
8. Huang MW, Wu WJ, Lyv XM et al. The role of ^{125}I interstitial brachytherapy for inoperable parotid gland carcinoma. *Brachytherapy* 2018;17:244–9.
9. Xu N, Zheng L, Wu WJ et al. Definitive ^{125}I brachytherapy of locally advanced adenoid cystic carcinoma involving the Skull Base with satisfying efficacy and safety. *J Oral Maxillofac Surg* 2019;77:2143–53.
10. Huang MW, Liu SM, Zheng L et al. A digital model individual template and CT-guided ^{125}I seed implants for malignant tumors of the head and neck. *J Radiat Res* 2012;53:973–7.
11. Huang MW, Zhang JG, Zheng L et al. Accuracy evaluation of a 3D-printed individual template for needle guidance in head and neck brachytherapy. *J Radiat Res* 2016;57:662–7.
12. Du W, Chen G, Bai D et al. Treatment of skeletal open bite using a navigation system: CAD/CAM osteotomy and drilling guides combined with pre-bent titanium plates. *Int J Oral Maxillofac Surg* 2019;48:502–10.
13. Ewers R, Schicho K, Undt G et al. Basic research and 12 years of clinical experience in computer-assisted navigation technology: a review. *Int J Oral Maxillofac Surg* 2005;34:1–8.
14. Hasan W, Daly M, Chan H et al. Intraoperative cone-beam CT-guided osteotomy navigation in mandible and maxilla surgery. *Laryngoscope* 2020;130:1166–72.
15. Casap N, Wexler A, Eliashar R. Computerized navigation for surgery of the lower jaw: comparison of 2 navigation systems. *J Oral Maxillofac Surg* 2008;66:1467–75.
16. Cleary K, Peters T. Image-guided interventions: technology review and clinical applications. *Annu Rev Biomed Eng* 2010;12:119–42.
17. Ji Z, Jiang Y, Sun H et al. 3D-printed template and optical needle navigation in CT-guided iodine-125 permanent seed implantation. *J Contemp Brachytherapy* 2021;13:410–8.
18. Zhang GH, Lyv XM, Wu WJ et al. Evaluation of the accuracy of computer-assisted techniques in the interstitial brachytherapy of the deep regions of the head and neck. *Brachytherapy* 2019;18:217–23.
19. Fan Y, Huang MW, Zheng L et al. Three-dimensional verification of ^{125}I seed stability after permanent implantation in the parotid gland and periparotid region. *Radiat Oncol* 2015;10:242.
20. Nath R, Bice W, Butler W et al. AAPM recommendations on dose prescription and reporting methods for permanent interstitial brachytherapy for prostate cancer: report of task group 137. *Med Phys* 2009;36:5310–22.
21. Lee L, Damato A, Viswanathan A. Clinical outcomes of high-dose-rate interstitial gynecologic brachytherapy using real-time CT guidance. *Brachytherapy* 2013;12:303–10.
22. de Arcos J, Schmidt E, Wang W et al. Prospective clinical implementation of a novel magnetic resonance tracking device for real-time brachytherapy catheter positioning. *Int J Radiat Oncol Biol Phys* 2017;99:618–26.
23. Kobayashi T, Kaneko M, Sumi M et al. CT-assisted transbronchial brachytherapy for small peripheral lung cancer. *Jpn J Clin Oncol* 2000;30:109–12.
24. Harms W, Krempien R, Grehn C et al. Electromagnetically navigated brachytherapy as a new treatment option for peripheral pulmonary tumors. *Strahlenther Onkol* 2006;182:108–11.
25. Krempien R, Hassfeld S, Kozak J et al. Frameless image guidance improves accuracy in three-dimensional interstitial brachytherapy needle placement. *Int J Radiat Oncol Biol Phys* 2004;60:1645–51.
26. Ren Y, Bu R, Zhang L et al. Implantation of radioactive particles into the cranial base and orbital apex with the use of a magnetic resonance imaging-based surgical navigation system. *Oral Surg Oral Med Oral Pathol Oral Radiol* 2013;116:e473–7.
27. Cormack R, Tempany C, D'Amico A. Optimizing target coverage by dosimetric feedback during prostate brachytherapy. *Int J Radiat Oncol Biol Phys* 2000;48:1245–9.
28. Fan Y, Huang MW, Zhao YJ et al. Radioactive seed migration following parotid gland interstitial brachytherapy. *Brachytherapy* 2017;16:1219–24.